Journal of Materials Chemistry A

PAPER

View Article Online
View Journal | View Issue

Cite this: J. Mater. Chem. A, 2015, 3, 24532

Selectively actuated multi-shape memory effect of a polymer multicomposite†

Wenbing Li,[a] Yanju Liu[b] and Jinsong Leng*[a]

Received 23rd October 2015
Accepted 6th November 2015

DOI: 10.1039/c5ta08513f

www.rsc.org/MaterialsA

In this paper, a new type of multicomposite styrene-based shape memory polymer (SSMP) was fabricated. This new SSMP included three regions: a SSMP matrix filled with multiwalled carbon nanotubes (SSMP–CNT), a SSMP matrix filled with Fe_3O_4 nanoparticles (SSMP–Fe_3O_4), and a third neat SSMP region which is located between the two composite regions. Differential scanning calorimetry (DSC) and dynamic mechanical analysis (DMA) results demonstrated that all the three SSMP materials possessed two well-separated transitions, which were subsequently used for the fixing/recovery of two temporary shapes (triple-shape memory effect) in each region. Furthermore, the unique selective actuation functionality of the multicomposite was demonstrated, based on the principle that Fe_3O_4 nanoparticles and CNT can selectively induce heat in a 30 kHz alternating magnetic field and 13.56 MHz radiofrequency, respectively. Therefore, well-controlled multiple shape recoveries of the multicomposite SSMP were achieved by applying selective stimuli. This proposed approach of selective actuations can be applied to other stimuli-responsive material systems to generate complex structures for target applications.

1. Introduction

Shape memory polymers (SMPs) are an exciting kind of stimuli-responsive material that has the capability to change from a temporary shape to a memorized permanent shape upon application of an external stimulus. With regard to triggering mechanisms, the shape memory effect has been triggered by direct heating,[1–3] magnetic field,[4–7] electricity,[8] light[9] and moisture stimulus.[10,11] Due to their unique ability, SMPs have been applied in various fields, such as space deployable structures,[12] artificial muscles,[13] smart actuators,[14] self-healing systems,[15] minimally invasive surgical sutures,[16] tissue engineering scaffolds,[17] active assembly/disassembly,[18,19] information carriers,[20,21] and textiles.[22,23]

Most SMPs are dual-shape memory polymers that have only one permanent shape and one temporary shape.[24,25] The dual-shape memory effect is based on a single transition (a glass transition or a melting transition) to fix the temporary shape after a programming step. Compared with the traditional dual-shape memory polymers, multi-shape memory polymers are able to memorize more shapes.[2] Taking triple-shape memory polymers as an example, there are two strategies to achieve a triple-shape memory effect (TSME): the first one is the utilization of a SMP with a broad transition temperature;[26,27] the second approach uses two distinct transition temperatures to obtain a TSME.[28–32] Besides, currently known dual- and multi-shape memory polymers are capable of recovering by direct heating[33,34] or remote triggering.[35,36] Considering the actuation mechanism, all the known conventional SMPs can recover totally with one stimulus, but cannot recover controllably with selective stimuli. The application of these SMPs, therefore, is limited by the number of temporary shapes they can memorize and the form to recover the temporary shapes in the face of ever-increasing complex demands. Herein, multifunctional SMPs[37,38] will gradually become a research hotspot due to their ability to process complex deformation as requested and the broad application prospects.

In this study, we reported a multicomposite with a multi-shape memory effect including three regions: a neat styrene-based shape memory polymer (neat SSMP) segment as the center segment; Fe_3O_4 nanoparticles as a magnetism-responsive source were composited with the styrene-based shape memory polymer (SSMP–Fe_3O_4) to construct the first segment;

[a]Centre for Composite Materials and Structures, Harbin Institute of Technology (HIT), No. 2 YiKuang Street, PO Box 3011, Harbin 150080, PR China. E-mail: lengjs@hit.edu.cn

[b]Department of Astronautical Science and Mechanics, Harbin Institute of Technology (HIT), Harbin 150080, PR China

† Electronic supplementary information (ESI) available: Tensile results and Young's modulus values of neat SSMP, SSMP–Fe_3O_4 and SSMP–CNT samples (Fig. S1), the dual-shape memory recovery process of SSMP–Fe_3O_4 and SSMP–CNT samples (Fig. S2), the triple-shape memory recovery process of SSMP–Fe_3O_4 and SSMP–CNT samples (Fig. S3), infrared images of the multicomposite sample during recovery in an alternating magnetic field (Fig. S4), mechanical properties of neat SSMP, SSMP–Fe_3O_4 and SSMP–CNT samples (Table S1), alternating magnetic field inducing the shape memory recovery process (Movie S1), radiofrequency inducing the shape memory recovery process (Movie S2) and the direct heating inducing shape memory recovery process (Movie S3). See DOI: 10.1039/c5ta08513f

a radiofrequency-responsive multiwalled carbon nanotube embedded SSMP (SSMP–CNT) was employed to form the third segment. The fabricated shape memory polymer can exhibit a shape memory effect under remote control and selective triggering. Unlike conventional shape memory recovery, herein, the multicomposite can recover the multiple temporary shapes by selective actuations, due to the fact that Fe_3O_4 and CNTs can induce independent heat in an alternating magnetic field (30 kHz frequency) and radiofrequency (RF) (13.56 MHz frequency), respectively.[6,37] When exposed to the two different fields (30 kHz alternating magnetic field and 13.56 MHz RF), only the corresponding section can be heated independently. With such a method, well-controlled multiple shape recoveries can be achieved.

2. Experimental section

Materials

Based on our previous literature,[39] the styrene-based shape memory polymer was synthesized by using Sigma-Aldrich (St. Louis, MO, USA) chemicals which consisted of styrene, a vinyl compound, polystyrene, and a cross-linking agent (bifunctional monomer). Benzoperoxide was used as the reaction initiator. Fe_3O_4 nanoparticles with a diameter of about 20 nm were synthesized on the basis of a chemical co-precipitation method as described in our previous reports.[40] Multiwalled carbon nanotubes (carboxyl functionalized) with a diameter of 20–30 nm and a length about 30 μm were purchased from Chengdu Institute of Organic Chemistry, Chinese Academy of Sciences. All other chemicals and solvents were of reagent grade or better and used without further purification.

SSMP nanocomposite synthesis

Firstly, pre-weighed nanoparticles (Fe_3O_4 or CNT) were dispersed in the neat SSMP by ultrasonication for 10 min. Then the obtained mixture was further mixed by using a vortex mixer for 1 min before being polymerized between two glass plates with Teflon linings, separated by a 2 mm spacer. The polymerization temperature was 75 °C, and the reaction time was 24 h. After polymerization, the samples were obtained for follow-up characterization and shape memory evaluation.

Multicomposite SSMP synthesis

The multicomposite SSMP was synthesized according to the following three steps. Firstly, the SSMP–Fe_3O_4 monomer solution was partially cured for 30 min. Then, the neat SSMP monomer solution was added on top of the first region and was also partially cured for 30 min. Finally, the SSMP–CNT monomer solution was added and fully cured for 24 h at 75 °C.

Characterization

The morphology of the Fe_3O_4, CNT and the dispersion of the two nanoparticles in the SSMP matrix were observed by using a scanning electron microscope (SEM, Quanta200, FEI, America), and the two different nanocomposite samples were both freeze-fractured in liquid nitrogen for the observation of the cross-sections with SEM. Thermal properties of the polymers were determined by differential scanning calorimetry (DSC, Q100, TA Instruments, America). In order to eliminate any unknown thermal history of the samples, heating and cooling were repeated from 0 °C to 140 °C. Also, the heating- and cooling-rate were both 20 °C min^{-1}. All the DSC data were obtained from the second heating process.

The dynamic mechanical analysis (DMA) data were obtained by using a DMA (SDTA861, Mettler-Toledo AG Analytical, Switzerland) in tensile resonant mode at a heating rate of 5 °C min^{-1} from 20 to 160 °C and at a frequency of 1 Hz. The storage modulus (E') and loss factor ($\tan\delta$) of the sample with a size of 20 mm × 3 mm × 2 mm (length × width × thickness) were tested. The static tensile test was completed by using a universal testing machine (Instron5567, Instron Co., America) with a cross-head speed of 1 mm min^{-1} at room temperature. The testing standard of the specimens was obtained from the tensile tests under the guidance of ASTM D638. The mechanical data were determined from the average of six tested specimens.

Shape memory evaluation

The shape fixity ratio (R_f) and recovery ratio (R_r) of the samples were evaluated by DMA (Q800, TA Instruments, America) using a controlled force mode according to our designed experiment. For the evaluation of shape memory properties, the SSMP samples were cut into cuboids (35 mm × 7 mm × 2 mm). The shape fixity ratio and recovery ratio were calculated according to the following equations:

$$R_f(0\rightarrow1) = \frac{\varepsilon_{f1}}{\varepsilon_{s1}} \times 100\% \quad (1)$$

$$R_f(1\rightarrow2) = \left(1 - \frac{\varepsilon_{s2} - \varepsilon_{f2}}{\varepsilon_{s2} - \varepsilon_{f1}}\right) \times 100\% \quad (2)$$

$$R_f(2\rightarrow1) = \left(\frac{\varepsilon_{s2} - \varepsilon_{s1,r}}{\varepsilon_{s2} - \varepsilon_{f1}}\right) \times 100\% \quad (3)$$

$$R_f(1\rightarrow0) = \left(1 - \frac{\varepsilon_{s0,r}}{\varepsilon_{f1}}\right) \times 100\% \quad (4)$$

The R_f and R_r of the triple-shape memory cycles were calculated by eqn (1) to (4).

Multi-shape recovery demonstration

Firstly, a multicomposite sample (120 mm × 5 mm × 2 mm) in straight strip form was heated at 130 °C for 10 minutes in an oven. Then the three sections of the sample were manually deformed to the "ʒ" shape by an external force. Secondly, the pre-deformed shape was fixed upon cooling to room temperature (about 20 °C). Finally, the specimen could go through a three-step shape memory recovery subjected to an alternating magnetic field of 30 kHz, RF field of 13.56 MHz, and direct oven heating, respectively.

3. Results and discussion

Characterization of the multicomposite SSMP

The SSMP matrixes were polymerized in the presence of nanofillers (Fe_3O_4 or CNT). The actual content (weight percentage of the SSMP) of Fe_3O_4 or CNTs was 5 wt% or 0.5 wt%, respectively. Also, a neat SSMP specimen was fabricated for the following test. The dispersion and morphology of nanoparticles in the SSMP composites were evaluated using scanning electron microscopy (SEM). From Fig. 1a and c, we can see that the Fe_3O_4 and CNT nanoparticles were both dispersed uniformly in the SSMP matrixes, but some agglomeration was observed at a higher magnification (Fig. 1b) for the SSMP–Fe_3O_4, nevertheless, the CNTs were individually dispersed in the SSMP–CNT (Fig. 1d). Herein, the conglomeration of Fe_3O_4 was due to the relatively high content and interactions among particles.

The differential scanning calorimetry (DSC) and dynamic mechanical analysis (DMA) were used to determine the glass transition temperatures (T_gs) of the SSMP composites and the neat SSMP. For all the three samples, two separate glass transitions can be observed in the DSC curves (Fig. 2). We observed that both the first and second T_g slightly increased with the introduction of CNTs and Fe_3O_4 nanoparticles. The reason may be the following two factors: firstly, interfacial interaction exists between the nanoparticles and SSMP matrix (shown in Fig. 1); secondly, the thermal motions of molecular chain segments of the SSMP are constrained by the two different particles.[41,42] Therefore, both CNTs and Fe_3O_4 particles play a very important role in these changes of T_g.

Fig. 3 shows the storage modulus (E') and loss factors (tan δ) of all the SSMP–CNT, SSMP–Fe_3O_4 composites and neat SSMP samples obtained by using DMA testing. The trends of DMA curves were also in good agreement with the DSC results in Fig. 2. A two-step significant modulus decrease in the temperature range below 60 °C as well as in the temperature range between 60 and 120 °C were observed in the DMA curves of the three samples. Hence, it was expected that the two-step modulus decrease could result in the release of deformed strain in two steps, and the three specimens (SSMP–CNT, SSMP–Fe_3O_4 and neat SSMP) could show two-step strain recovery behaviors.[43] Meanwhile, the tan δ curves sharply changed in the two different temperature ranges, and the two peaks of the tan δ *vs.* temperature curves were used to define the T_gs.[44,45] The results of the T_gs slightly increasing with the addition of CNTs and Fe_3O_4 nanoparticles accorded with those of DSC testing. Therefore, the introduction of CNTs and Fe_3O_4 into the SSMP matrix had a positive impact on the mechanical and shape memory properties of the composites.

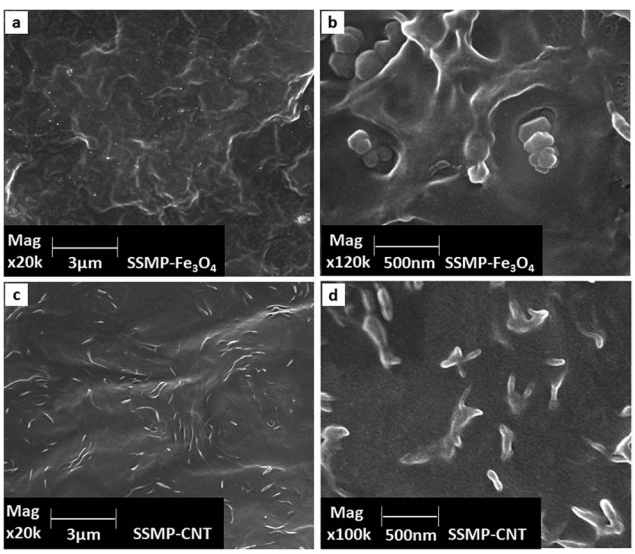

Fig. 1 SEM images of the SSMP composites: (a) SSMP–Fe_3O_4 at ×20 000 magnification; (b) SSMP–Fe_3O_4 at ×120 000 magnification; (c) SSMP–CNT at ×20 000 magnification; (d) SSMP–CNT at ×100 000 magnification.

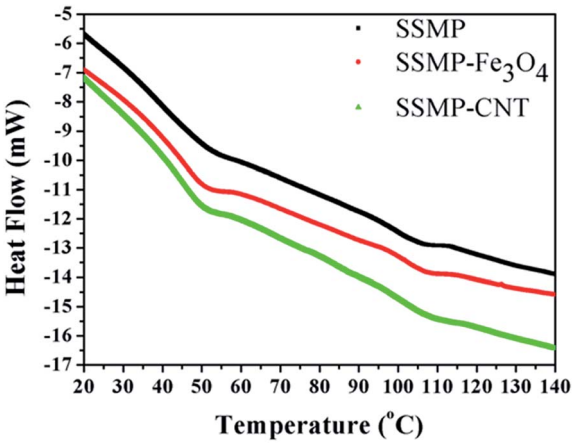

Fig. 2 DSC thermograms of the pure SSMP, SSMP–Fe_3O_4 and SSMP–CNT composites.

The mechanical properties of the three specimens were investigated in Fig. S1 in the ESI.† Fig. S1a† shows the typical stress–strain behavior at room temperature. From the results of stress–strain curves, the maximum tensile stress increased with introducing nanoparticles, and the SSMP–CNT composite presented a much better enhancement than the SSMP–Fe_3O_4 nanocomposite, reflecting the results of hardness. Meanwhile, the SSMP–CNT composite also possessed the best elongation at the break (nearly 140%). The reason could be that the nanofillers provide significant reinforcement of the SSMP, so the nanocomposites (SSMP–CNT, SSMP–Fe_3O_4) exhibit better thermal and mechanical properties than the unreinforced neat SSMP. Furthermore, the tube-shaped CNT nanofillers offer better reinforcement than spherical Fe_3O_4 nanoparticles, because of their high aspect ratio and ability to reinforce in multiple directions.[46] The Young's moduli (shown in Fig. S1b†) were calculated from the tensile curves. The results also demonstrated that the SSMP–CNT composite led to the best enhancement. This was also in good agreement with the tensile tests in Fig. S1a.†

Tensile test results at room temperature are presented in Table S1 in the ESI.† From this table, the nanocomposites showed an improvement in tensile strength and elongation at break. Such an increase was attributed to the enhancement of

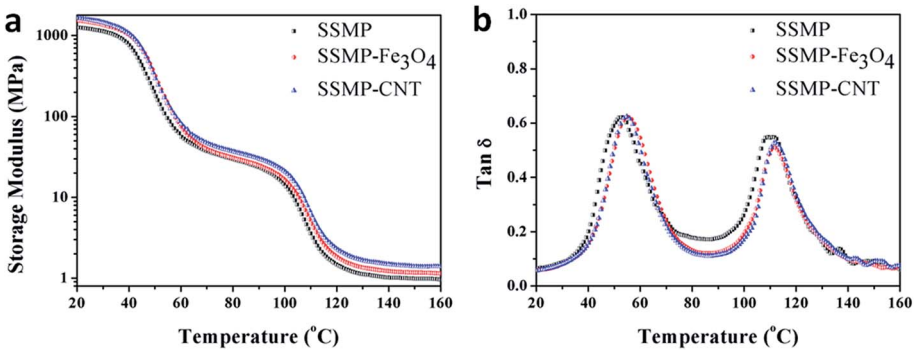

Fig. 3 (a) Storage modulus E' and (b) loss factor tan δ *vs.* temperature of the pure SSMP, SSMP–Fe_3O_4 and SSMP–CNT composites, measured by DMA.

interfacial bonding between the nanofillers and polymer chains. Additionally, the functional groups on the surface of nanoparticles potentially acted as a plasticizer, which contributed to dangling chain formation in the matrix, as reported by Aglan and Jana.[47,48]

Dual- and triple-shape memory properties

The typical dual-shape memory property of the neat SSMP was determined by using DMA as shown in Fig. 4a. According to the DSC and DMA results, the dual-shape memory recovery temperature was determined as 130 °C, so that the specimen could be totally softened. As shown in Fig. 4a, the sample was firstly heated at 130 °C for 5 minutes, and then it was strained at a constant stress to obtain a temporary shape, which was marked as ε_s. The pre-deformed shape was fixed by cooling to −20 °C, releasing the stress, and the strain was marked as ε_f. After keeping the temporary shape at −20 °C for 5 minutes, the specimen was reheated to 130 °C, recovering to the original shape, and the unrecovered strain was marked as ε_{ur}. The shape fixity ratio (R_f) was defined as $\varepsilon_f/\varepsilon_s$. The shape recovery ratio (R_r) was defined as $\varepsilon_f - \varepsilon_{ur}/\varepsilon_f$. Therefore, the R_f and R_r of the dual-shape memory cycle were calculated, and the value of R_f and R_r was 97% and 95%, respectively.

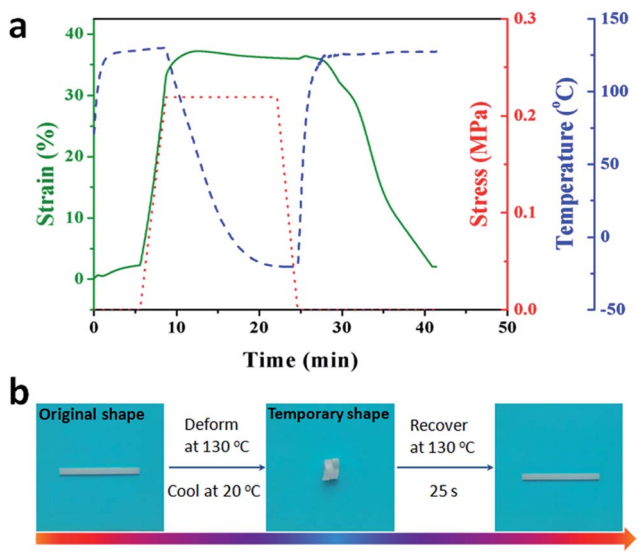

Fig. 4 Quantitative demonstration of dual-shape memory properties of pure SSMP with DMA (a); qualitative process of dual-shape memory fixing and recovery (b).

Fig. 4b shows the macroscopic dual-shape memory recovery process of the neat SSMP stripe-shaped specimen with a size of 60 mm × 5 mm × 2 mm (length × width × thickness) in the oven. Firstly, the specimen was heated at 130 °C for 5 minutes, and then deformed to a temporary spiral shape, and cooled to 20 °C, releasing the stress and fixing the temporary shape at last. When heating the specimen again to 130 °C, the temporary spiral shape could recover its original shape in 25 s. In addition, the visual dual-shape memory recovery demonstration of the SSMP–Fe_3O_4 and SSMP–CNT is shown in Fig. S2a and b in the ESI,† respectively.

From the results of DSC and DMA, we can clearly find that both the neat SSMP and nanocomposites (SSMP–CNT and SSMP–Fe_3O_4) have two distinct transition temperatures (nearly 50 °C and 110 °C) which could endow them with a good triple shape memory effect.[49] Herein, the first transition at the lower temperature can be referenced in our previous literature,[39] and the higher thermal transition attributed to the glass transition of polystyrene. A similar result can be found in the previous report.[32] Taking neat SSMP as an example, the quantitative demonstration of triple-shape memory capabilities is shown in Fig. 5a, where the stress–strain–temperature curves were obtained by using DMA testing. Firstly, the specimen was stretched at 130 °C to obtain a temporary shape 1 which was marked as ε_{s1}, then cooled to 75 °C, releasing the stress and fixing the strain which was marked as ε_{f1}. The strain clearly decreased after unloading at 75 °C, but a partial vitrification of "soft domains" could be concluded as previously reported,[26] and this "frozen" part contributed to the fixation of the temporary shape. Secondly, the specimen was further stretched at 75 °C to obtain another temporary shape 2 which was marked as ε_{s2}, and then cooled down to −20 °C to fix the second strain, marked as ε_{f2}. Lastly, the sample was unloaded and heated again to 75 °C, the specimen could recover to temporary shape 1, the strain was marked as $\varepsilon_{s1,r}$. Later when further reheated to 130 °C, the specimen could recover to the initial shape, and the

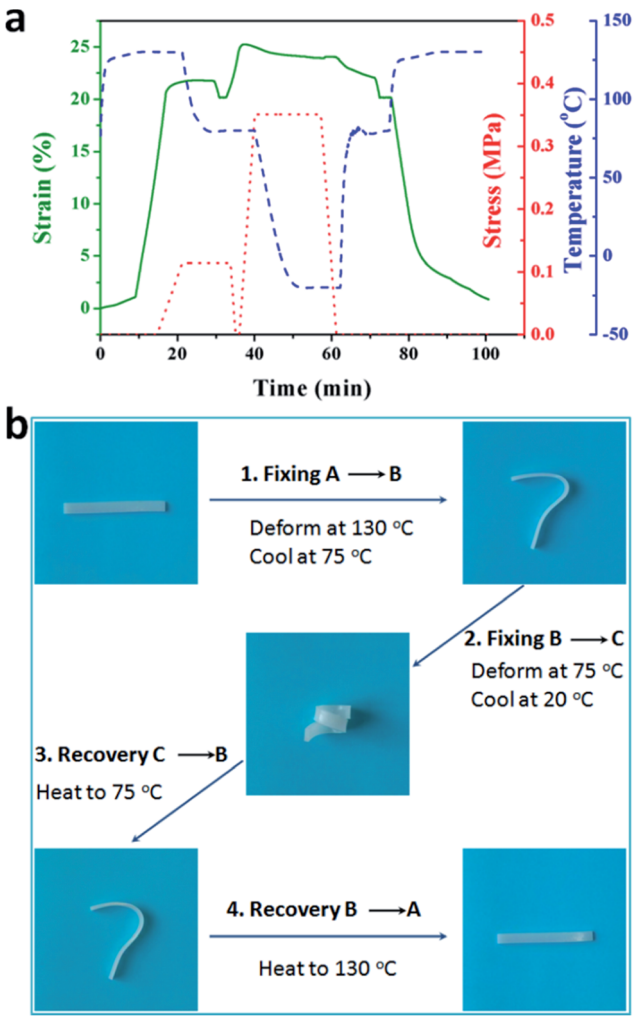

Fig. 5 Quantitative demonstration of triple shape memory properties of pure SSMP with DMA (a); qualitative process of triple shape memory fixing and recovery (b).

strain was marked as $\varepsilon_{s0,r}$. The observed two-step recovery behavior is due to the fact that the polystyrene component can only partially resist the matrix recovery. That is, if the polystyrene component could resist all the matrix recovery, the first recovery at 75 °C would not have been noticed.[32] Eqn (1)–(4) were used to calculate the R_f and R_r for the triple-shape memory cycles. The R_f $(0 \rightarrow 1)$ and R_f $(1 \rightarrow 2)$ reach 93% and 95%, respectively, and the R_r $(2 \rightarrow 1)$ and R_r $(1 \rightarrow 0)$ could reach 99% and 93% respectively.

The triple-shape memory effect is further demonstrated visually in Fig. 5b. The strip-shaped sample with a size of 60 mm × 5 mm × 2 mm (length × width × thickness) was deformed to a temporary "7" shape (shape B) at 130 °C and fixed at 75 °C for 1 minute, then the sample was further deformed to a spiral shape (shape C) at 75 °C and fixed at 20 °C for 1 minute. When the temporary shape C was placed in the oven at 75 °C for 6 s, it could recover to the shape B, and the temporary shape B could recover its original shape after placing in the oven at 130 °C for 20 s. Thus, increases of entropy by regaining the segmental motion above the first T_g and the second T_g are distinctly separated so that macroscopic triple-shape memory behavior of the neat SSMP is accessible.[50] Fig. S3a and b in the ESI† provide a series of photographs showing the macroscopic triple-shape memory recovery process of the SSMP–Fe_3O_4 and SSMP–CNT.

Multiple temporary shapes recovery of the multicomposite SSMP

In order to achieve the selective recovery of the shape memory polymer, the multicomposite specimen, which consists of a SSMP–Fe_3O_4 zone, a neat SSMP zone and a SSMP–CNT zone, was fabricated. And the detailed fabrication procedure is given in the Experimental section. During the three-step synthesis of the multicomposite SSMP, the unreacted functional groups (double bonds) on the surface of the first cured region continued to react with the second monomer solution that was poured onto it, which produced a strong interface. The interface between the second region and the third region was the same. A multicomposite sample with a straight strip shape was manually deformed to the "ʒ" shape (temporary shape 1) in the three zones by an external force, and the selective recovery is demonstrated in Fig. 6. Firstly, the deformed specimen was placed in a 30 kHz alternating magnetic field, but only the SSMP–Fe_3O_4 zone was heated and could recover to temporary shape 2. The shape memory recovery process of SSMP–Fe_3O_4 is shown in Movie S1 in the ESI.† When subsequently placed in a 13.56 MHz RF field, the zone of SSMP–CNT was selectively heated and recovered to temporary shape 3, and the corresponding recovery process of SSMP–CNT is demonstrated in Movie S2 in the ESI.† Finally, after heating in an oven at 130 °C, the neat SSMP zone was heated and recovered (shown in Movie S3 in the ESI†). Throughout this entire process, the three temporary shapes were selectively actuated and recovered, hence, realizing the controllability of the shape memory recovery.

The nature of shape memory induced by an alternating magnetic field or a RF field is thermo-induced.[6,37] Considering

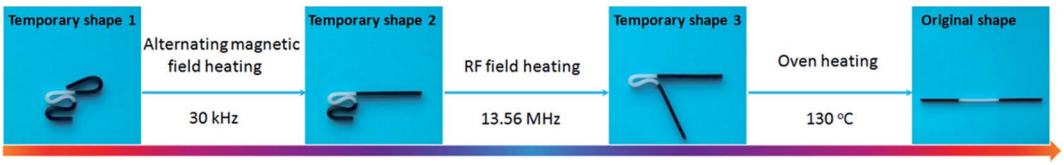

Fig. 6 Experimental demonstration of the selective shape memory recovery. The sample was subjected to an alternating magnetic field of 30 kHz, a RF field of 13.56 MHz and direct oven heating at 130 °C sequentially.

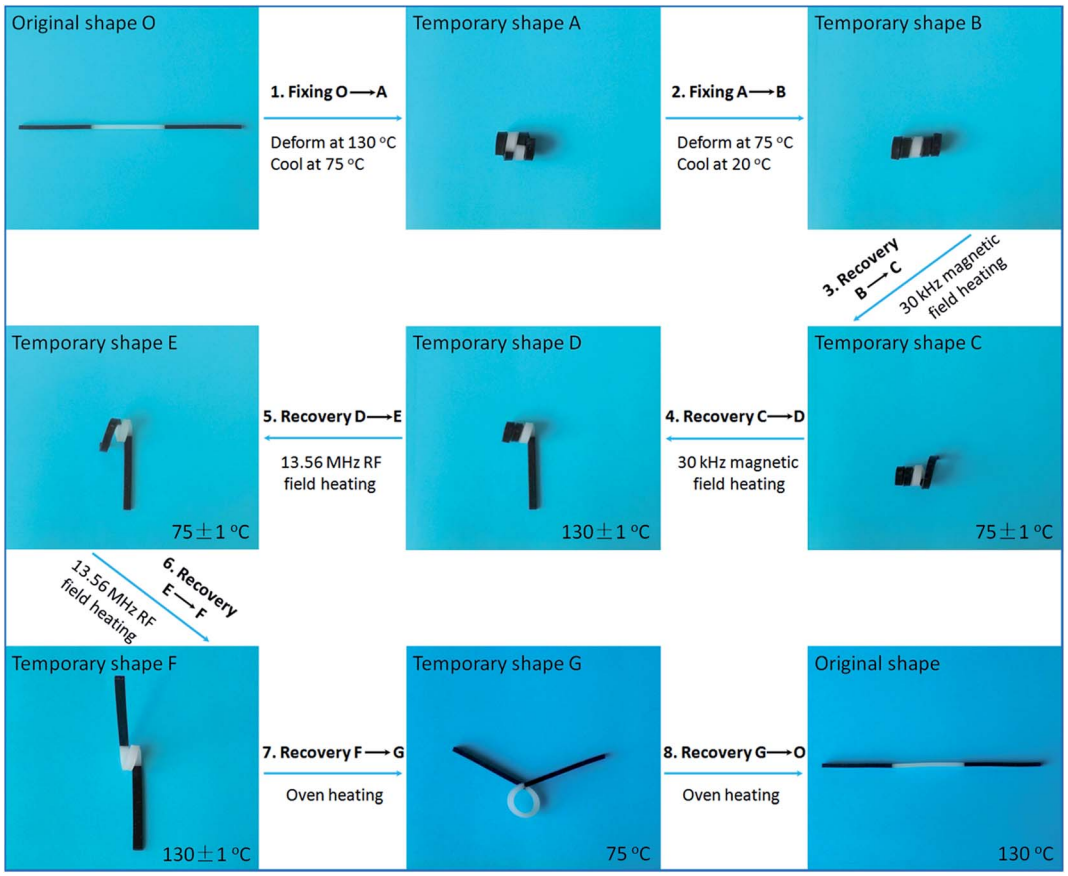

Fig. 7 Series of digital photographs showing selective multiple shape recovery processes of the multicomposite sample in an alternating magnetic field of 30 kHz first, in a RF field of 13.56 MHz second and in the oven (75 °C and 130 °C, respectively) last.

the alternating magnetic field as an instance, Fig. S4 in the ESI† shows the temperature distribution of the multicomposite sample in an alternating magnetic field monitored using an infrared camera. When the alternating magnetic field was applied, the inductive heating resulted in a gradually increased temperature. This was because Brownian and Néel relaxation losses of Fe_3O_4 could be transferred into heat.[6] The SSMP–Fe_3O_4 region recovered to its original shape after 175 s since the application of the alternating magnetic field, and its temperature could reach about 130 °C.

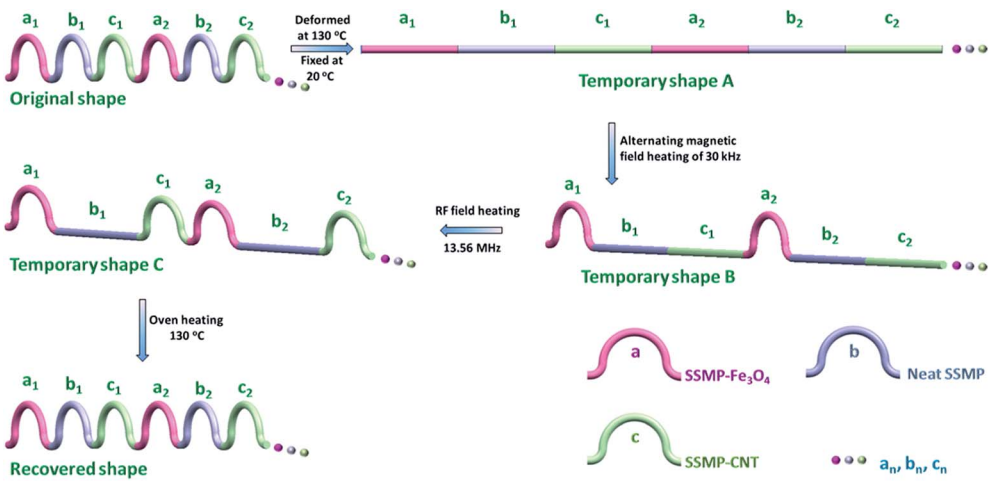

Scheme 1 Schematic of the selective shape recoveries of the multicomposite SSMP induced by alternating magnetic field heating, RF field heating and oven heating, respectively (a_n, b_n and c_n stand for the n sections of SSMP–Fe_3O_4, neat SSMP and SSMP–CNT, respectively).

As all the neat SSMP, SSMP–Fe_3O_4 and SSMP–CNT had a triple-shape memory effect, every zone of the multicomposite straight strip specimen could be deformed for two temporary shapes. Fig. 7 shows the selective recovery of the seven pre-deformed shapes. A straight strip-shaped specimen (original shape O) was first deformed to temporary shape A at 130 °C in all three zones, then the deformed shape A was fixed in 75 °C, next the shape A was deformed to temporary shape B at 75 °C, and cooled at 20 °C to fix the shape. When the deformed specimen with shape B was subjected to a 30 kHz alternating magnetic field for 38 seconds, only the zone of SSMP–Fe_3O_4 was selectively heated and led to partial recovery (temporary shape C), then the heating was continued in a 30 kHz alternating magnetic field, the SSMP–Fe_3O_4 zone was completely recovered. After that the temporary shape D was obtained. Upon subsequently subjecting to a 13.56 MHz RF field for 36 seconds, the SSMP–CNT zone was selectively actuated and resulted in partial recovery (temporary shape E), when kept heating in a 13.56 MHz RF field, the zone of SSMP–CNT could completely recover. So, the temporary shape F was obtained. Finally, the neat SSMP zone recovered partially after being heated at 75 °C in an oven and obtained temporary shape G, when heating was proceeded at 130 °C, the neat SSMP zone could return to the original shape perfectly. In this whole process, the selective recovery of the seven temporary shapes was realized, indicating that selective actuations could realize the multiple shape recoveries, which was facile and could be controlled accurately. The previously reported thermo-responsive SMPs needed a broad thermo-mechanical transition temperature or several distinct transition temperatures to achieve a multi-shape memory effect.[49] However, in this paper, a simple multicomposite can exhibit an excellent multi-shape memory effect through selective stimuli.

Finally, further studies will be focused on the methods to fabricate excellent multicomposite SSMPs, such as four-section, five-section and so on. Scheme 1 shows the selective shape recovery processes of the multicomposite SSMP. Firstly, the wavy form was deformed to an "I" shape (temporary shape A) at 130 °C and fixed at 20 °C. After that, the temporary shape A was recovered to temporary shape B in a 30 kHz alternating magnetic field; the temporary shape B was recovered to temporary shape C in a 13.56 MHz RF field and the temporary shape C was restored after heating in a 130 °C oven. It is possible to conclude that the novel *n*-section material has promising characteristics to be used in biomimetic materials.

4. Conclusions

In summary, we successfully fabricated a novel multicomposite SSMP which consisted of three parts: a SSMP–Fe_3O_4 zone, a neat SSMP zone and a SSMP–CNT zone, and the materials of the three regions all had an excellent triple-shape memory effect. In this system, the SSMP–Fe_3O_4 and SSMP–CNT region could be actuated remotely in the 30 kHz alternating magnetic field and 13.56 MHz RF field, respectively. The results of the selective actuations and triple-shape memory property indicated that the multicomposite SSMP possessed a well-controlled multiple temporary shape recovery capability. Besides the demonstrated unique performance in the form of selective actuations for our multicomposite SSMP, it is significant that this driving approach affords great actuation flexibility that can be used to design stimuli-responsive material systems for target applications. For instance, through imprint lithography, such multicomposite SSMPs with controllable shape memory behavior can be prepared into a programmable pattern-memorizing surface that can be used as micro-optics.

Acknowledgements

This work has been financially supported by the National Nature Science Foundation of China (Grant no. 11225211), for which we are very grateful. The authors thank Ms Y. Li for her kind support in the material characterization.

Notes and references

1 M. Behl and A. Lendlein, *Mater. Today*, 2007, **10**, 20–28.
2 T. Xie, *Nature*, 2010, **464**, 267–270.
3 J. Xu and J. Song, *Proc. Natl. Acad. Sci. U. S. A.*, 2010, **107**, 7652–7657.
4 M. Y. Razzaq, M. Behl and A. Lendlein, *Adv. Funct. Mater.*, 2012, **22**, 184–191.
5 R. Mohr, K. Kratz, T. Weigel, M. Lucka-Gabor, M. Moneke and A. Lendlein, *Proc. Natl. Acad. Sci. U. S. A.*, 2006, **103**, 3540–3545.
6 X. Yu, S. Zhou, X. Zheng, T. Guo, Y. Xiao and B. Song, *Nanotechnology*, 2009, **20**, 235702.
7 X. Zheng, S. Zhou, Y. Xiao, X. Yu, X. Li and P. Wu, *Colloids Surf., B*, 2009, **71**, 67–72.
8 J. Leng, X. Lan, Y. Liu and S. Du, *Prog. Mater. Sci.*, 2011, **56**, 1077–1135.
9 A. Lendlein, H. Jiang, O. Jünger and R. Langer, *Nature*, 2005, **434**, 879–882.
10 S. Chen, J. Hu, C. Yuen and L. Chan, *Polymer*, 2009, **50**, 4424–4428.
11 W. Wang, H. Lu, Y. Liu and J. Leng, *J. Mater. Chem. A*, 2014, **2**, 5441–5449.
12 X. Lan, Y. Liu, H. Lv, X. Wang, J. Leng and S. Du, *Smart Mater. Struct.*, 2009, **18**, 24002.
13 T. Chung, A. Romo-Uribe and P. T. Mather, *Macromolecules*, 2008, **41**, 184–192.
14 M. Behl, K. Kratz, U. Noechel, T. Sauter and A. Lendlein, *Proc. Natl. Acad. Sci. U. S. A.*, 2013, **110**, 12555–12559.
15 X. C. Xiao, T. Xie and Y. T. Cheng, *J. Mater. Chem.*, 2010, **20**, 3508–3514.
16 A. Lendlein and R. Langer, *Science*, 2002, **296**, 1673–1676.
17 S. Neuss, I. Blomenkamp, R. Stainforth, D. Boltersdorf, M. Jansen, N. Butz, A. Perez-Bouza and R. Knüchel, *Biomaterials*, 2009, **30**, 1697–1705.
18 L. Sun, W. M. Huang, H. B. Lu, C. C. Wang and J. L. Zhang, *Assemb. Autom.*, 2014, **34**, 78–93.
19 H. Purnawali, W. W. Xu, Y. Zhao, Z. Ding, C. C. Wang, W. M. Huang and H. Fan, *Smart Mater. Struct.*, 2012, **21**, 75006.

20 M. Ecker and T. Pretsch, *RSC Adv.*, 2014, **4**, 46680–46688.
21 N. Fritzsche and T. Pretsch, *Macromolecules*, 2014, **47**, 5952–5959.
22 J. Hu, H. Meng, G. Li and S. I. Ibekwe, *Smart Mater. Struct.*, 2012, **21**, 53001.
23 J. Hu and S. Chen, *J. Mater. Chem.*, 2010, **20**, 3346–3355.
24 A. Lendlein and S. Kelch, *Angew. Chem., Int. Ed.*, 2002, **41**, 2034–2057.
25 K. Y. Mya, H. B. Gose, T. Pretsch, M. Bothe and C. He, *J. Mater. Chem.*, 2011, **21**, 4827–4836.
26 C. D. Samuel, S. Barrau, J. Lefebvre, J. Raquez and P. Dubois, *Macromolecules*, 2014, **47**, 6791–6803.
27 J. Li and T. Xie, *Macromolecules*, 2011, **44**, 175–180.
28 T. Pretsch, *Smart Mater. Struct.*, 2010, **19**, 15006.
29 I. Bellin, S. Kelch, R. Langer and A. Lendlein, *Proc. Natl. Acad. Sci. U. S. A.*, 2006, **103**, 18043–18047.
30 Y. Bai, X. Zhang, Q. Wang and T. Wang, *J. Mater. Chem. A*, 2014, **2**, 4771–4778.
31 J. Zhao, M. Chen, X. Wang, X. Zhao, Z. Wang, Z. Dang, L. Ma, G. Hu and F. Chen, *ACS Appl. Mater. Interfaces*, 2013, **5**, 5550–5556.
32 X. Luo and P. T. Mather, *Adv. Funct. Mater.*, 2010, **20**, 2649–2656.
33 C. M. Yakacki, R. Shandas, D. Safranski, A. M. Ortega, K. Sassaman and K. Gall, *Adv. Funct. Mater.*, 2008, **18**, 2428–2435.
34 M. Bothe, K. Y. Mya, E. M. J. Lin, C. C. Yeo, X. Lu, C. He and T. Pretsch, *Soft Matter*, 2012, **8**, 965–972.
35 H. Koerner, G. Price, N. A. Pearce, M. Alexander and R. A. Vaia, *Nat. Mater.*, 2004, **3**, 115–120.
36 U. N. Kumar, K. Kratz, W. Wagermaier, M. Behl and A. Lendlein, *J. Mater. Chem.*, 2010, **20**, 3404–3415.
37 Z. He, N. Satarkar, T. Xie, Y. T. Cheng and J. Z. Hilt, *Adv. Mater.*, 2011, **23**, 3192–3196.
38 M. Y. Razzaq, M. Behl, K. Kratz and A. Lendlein, *Adv. Mater.*, 2013, **25**, 5730–5733.
39 J. Leng, D. Zhang, Y. Liu, K. Yu and X. Lan, *Appl. Phys. Lett.*, 2010, **96**, 111905.
40 W. Li, Y. Liu and J. Leng, *RSC Adv.*, 2014, **4**, 61847–61854.
41 M. Abdalla, D. Dean, D. Adibempe, E. Nyairo, P. Robinson and G. Thompson, *Polymer*, 2007, **48**, 5662–5670.
42 H. Gu, S. Tadakamalla, Y. Huang, H. A. Colorado, Z. Luo, N. Haldolaarachchige, D. P. Young, S. Wei and Z. Guo, *ACS Appl. Mater. Interfaces*, 2012, **4**, 5613–5624.
43 S. Chen, J. Hu, C. W. Yuen, L. Chan and H. Zhuo, *Polym. Adv. Technol.*, 2010, **21**, 377–380.
44 N. C. Bleach, S. N. Nazhat, K. E. Tanner, M. Kellomäki and P. Törmälä, *Biomaterials*, 2002, **23**, 1579–1585.
45 X. Zheng, S. Zhou, X. Li and J. Weng, *Biomaterials*, 2006, **27**, 4288–4295.
46 B. Xu, Y. Q. Fu, M. Ahmad, J. K. Luo, W. M. Huang, A. Kraft, R. Reuben, Y. T. Pei, Z. G. Chen and J. T. M. de Hosson, *J. Mater. Chem.*, 2010, **20**, 3442–3448.
47 S. Ganguli, H. Aglan and D. Dean, *J. Elastomers Plast.*, 2005, **37**, 19–35.
48 F. Cao and S. C. Jana, *Polymer*, 2007, **48**, 3790–3800.
49 Q. Ge, X. Luo, C. B. Iversen, P. T. Mather, M. L. Dunn and H. J. Qi, *Soft Matter*, 2013, **9**, 2212–2223.
50 S. K. Ahn and R. M. Kasi, *Adv. Funct. Mater.*, 2011, **21**, 4543–4549.